FERMILAB
MAR 7 1996
LIBRARY

# PREPRINTS

# of the

# STEWARD OBSERVATORY

THE UNIVERSITY OF ARIZONA
TUCSON, ARIZONA 85721 U.S.A.

STEWARD-1319

No. 1319

## THE BIG PICTURE FROM RADIO WAVES TO GAMMA RAYS

C. D. Impey

Steward Observatory,
The University of Arizona
Tucson, Arizona 85721, U.S.A.

Contributions to IAU Symposium 175
"Extragalactic Radio Sources"

| NAME | I D No. | M.S. |
|---|---|---|
| | | |
| | | |
| | | |
| | | |
| | | |
| | | |
| | | |
| | | |
| | | |
| | | |

RETURN TO FERMILAB LIBRARY

Fermilab Library
0 1160 0050791 7

# THE BIG PICTURE FROM RADIO WAVES TO GAMMA RAYS

C.D. IMPEY
*Steward Observatory*
*University of Arizona, Tucson, AZ 85721, USA*

## 1. Introduction

The conventional paradigm of active galactic nuclei (AGN) holds that they are powered by accretion onto a gravitational engine. In addition, the presence of Doopler-boosted radiation from jets and anisotropic obscuration can create large differences between the observed and intrinsic properties of AGN (Antonucci 1994). The "big picture"of extragalactic radio sources must include observations across the electromagnetic spectrum. Relativistic processes produce radiation with a very wide bandwidth. In addition, much of the energy from AGN is reprocessed, and the opacity is a function of wavelength. Finally, it turns out that only a small fraction of the bolometric luminosity of most AGN is emitted in the traditional radio and optical bands.

## 2. Quasars and Blazars

Samples of strong radio sources selected at high frequencies have the best complementary information at other wavelengths. For example, the roughly 300 quasars in the Kühr (1981) catalog now have virtually complete redshift information. In addition, about 70% of the quasars have optical polarimetry. After controlling for luminosity, strong optical and far infrared emission is correlated with the compactness of the radio source. High optical polarization, a clear indicator of nonthermal emission, is strongly correlated with radio compactness. Sources with these collective properties are called "blazars." It is also possible to distinguish highly polarized quasars, where normal quasar broad lines are superimposed on a polarized continuum, and BL Lac objects, where the lines are weak or absent. Among quasars stronger than 1 Jy at 5 GHz, the proportion of highly polarized objects falls from

60% at $z = 0.3$ to just under 20% at $z = 2.7$. The BL Lac fraction in the 1 Jy catalog falls more steeply, from 30% at $z = 0.3$ to under 10% at $z = 1.5$.

These observations can be explained by a model where the radio and optical emission is beamed with a similar Lorentz factor and geometry, presuming that the optical emission is a sum of power law synchrotron and thermal accretion disk components. The decline in the fraction of highly polarized objects with increasing redshift results from the larger fraction of the emission which is due to the hot thermal component in the optical passband. This simple model works well for a power law spectral index of $\alpha = -1.5$, where $S_\nu \propto \nu^\alpha$. As expected, low polarization quasars are brighter than high polarization quasars, and radio-to-optical spectral index steepens with redshift, due to the dependence of the beamed power on local spectral index. BL Lac objects form a distinct class. No thermal components are seen, even at minimum light, so the rapid decline in redshift must be intrinsic to the population. Compact radio structure is an excellent predictor of nonthermal optical/infrared properties.

## 3. Strong Gamma Ray Emission

Gamma ray emssion has been detected from a significant number of AGN (Montigny et al. 1995); over half of the sources at high galactic latitude in the second EGRET catalog are associated with strong radio sources, typically blazars (Thompson et al. 1995). About 35 of these firm identifications are in the 1 Jy sample. When the spectral energy distributions are normalized to the radio band, it is found that the gamma ray flux is much more closely correlated with the radio flux than with the optical or ultraviolet flux. This may favor models where gamma ray photons are multiply upscattered from much lower energies, rather than from optical/UV seed photons. The correlation between radio flux, $S_r$, and (non-simultaneous) gamma ray flux, $S_\gamma$, is weak but significant. The ratio $S_\gamma/S_r$ is influenced by the large number of upper limits, but the 95% confidence range is $0.0038 < S_\gamma/S_r < 0.018$. Integrating the source counts, and taking account of variability, the contribution of AGN to the 100 MeV background is $46^{+54}_{-23}$%. Given the radio weakness of the more ubiquitous optically selected quasar, they must contribute less than 5% of the gamma ray background.

This work was partially supported by NSF grant AST 93-20715.

Antonucci, R.R. 1994, Ann.Rev.Ast.Ap., 31, 473
Kühr, H. et al. 1981, Ast.Ap.Supp., 45, 367
Montigny, C. et al. 1995, Ap.J., 440, 525
Thompson, D.J. et al. 1995, Ap.J.Supp., in press

# THE RADIO AND OPTICAL PROPERTIES OF QUASARS

C.D. IMPEY AND E.J. HOOPER
*Steward Observatory*
*University of Arizona, Tucson, AZ 85721, USA*

C.B. FOLTZ
*Multiple Mirror Telescope Observatory*
*University of Arizona, Tucson, AZ 85721, USA*

AND

P.C. HEWETT
*Institute of Astronomy*
*Madingley Road, Cambridge CB3 0HA, England*

## 1. Introduction

The relationship between the radio and optical emission of quasars was first studied using radio-selected objects, which generally had high radio luminosities due to the relatively low sensitivity limits of the surveys. More recently, radio follow-up observations have been made of optical surveys surveys in other wavebands. Taken together, the two survey methods have detected quasars with a range of over 6 orders of magnitude in radio luminosity. We report here new observations with the Very Large Array (VLA) of 103 quasars from the Large Bright Quasar Survey (LBQS), with absolute magnitudes in the range $-25 < M_{\rm B} < -23$ and redshifts in the range $0.2 < z < 1.1$. This can be combined with our previous LBQS observations (Paper I, Paper II) to yield 359 quasars, the largest sample of sensitive radio observations of optically-selected quasars in a single survey.

## 2. Results

First, the distribution of radio luminosity does not depend on absolute magnitude over most of the range of $M_{\rm B}$ in the LBQS. The radio-loud fraction remains constant at $\approx 10\%$ for $-28 < M_{\rm B} < -23$ but rises to $\approx 30\%$ at brighter absolute magnitudes. Second, the radio properties of the LBQS

quasars as a function of $M_B$ are consistent with the existence of two radio emission mechanisms, one correlated with optical luminosity, the other independent. The sudden decrease in radio-loud fraction for $M_B$ fainter than $-24$ observed in the Palomar-Greeen (PG) sample is not present in the expanded LBQS sample. A selection effect to which the LBQS is mostly immune is the likely cause of the decrease in the PG sample.

The radio-loud fraction in optically selected quasars appears to be unevolving at a value of $\approx 10\%$, aside from a modest increase at $z \sim 1$, from $z = 0.2$ to redshifts approaching 5, based on the LBQS and three high-$z$ optically selected samples. A model based on a radio luminosity function derived from radio-selected quasars (Dunlop & Peacock 1990) matches the data well, including the modest rise around $z = 1$, at all except the highest redshifts. The high radio-loud fraction in the PG sample remains unexplained (Kellerman et al. 1989). Fourth, the radio properties of the X-ray selected EMSS also differ from those of the LBQS (Stocke et al. 1991). The rapid rise in radio-loud fraction observed for $M_B \approx -24$ is primarily an evolutionary effect resulting from a well-established correlation between X-ray and radio luminosity. The rise in radio-loud fraction with redshift is also consistent with the observed correlation between radio and X-ray emission for faint radio sources (Brinkmann et al. 1995).

These results are surprising in terms of the standard paradigm of AGN energy production. The constancy of the radio luminosity distribution over more than two orders of magnitude in optical luminosity is unexpected in the context of the standard black hole model. The radio emission mechanism appears to be only weakly tied to the mass accretion rate which presumably drives the optical and near-UV emission. Also, the radio-loud fraction is essentially constant over 90% of the Hubble time, during which the epoch of quasar formation occurs, and the comoving space density declines by a factor of several hundred to the present value.

This work was supported by NSF grant AST 93-20715 and NASA grant NGT-51152, a NASA Graduate Student Fellowship (EJH).

Brinkmann, W., et al. 1995, Ast.Ap.Supp., 109, 147

Dunlop, J. S., & Peacock, J. A. 1990, M.N.R.A.S., 247, 19

Hooper, E. J., Impey, C. D., Foltz, C. B., & Hewett, P. C. 1995, Ap.J., 445, 62 (Paper II)

Kellermann, K. I., Sramek, R., Schmidt, M., Shaffer, D. B., & Green, R. 1989, A.J., 98, 1195 (PG)

Stocke, J. T., et al. 1991, Ap.J.Supp., 76, 813

Visnovsky, K. L., Impey, C. D., Foltz, C. B., Hewett, P. C., Weymann, R. J., & Morris, S. L. 1992, Ap.J., 391, 560 (Paper I)

STEWARD-1324

# PREPRINTS

# of the

# STEWARD OBSERVATORY

THE UNIVERSITY OF ARIZONA
TUCSON, ARIZONA 85721 U.S.A.

Fermilab Library
0 1160 0042480 8

No. 1324

## ACTIVITY AND RADIATIVE CHARACTERISTICS OF THE CENTRAL ENGINE IN THE GALACTIC CENTER

Fulvio Melia[1]
Physics and Astronomy Departments
The University of Arizona
Tucson, Arizona 85721

Arizona U.

FERMILAB
APR 26 1996
LIBRARY

[1]Presidential Young Investigator

Invited talk, to appear in the Proceedings of the Fourth ESO/CTIO Workshop: The Galactic Center, Ed. Roland Gredel.

Arizona Theoretical Astrophysics Preprint #96-7

# Activity and Radiative Characteristics of the Central Engine in the Galactic Center

F. Melia[1]

*Physics and Astronomy Departments, University of Arizona, Tucson, AZ 85721*

**Abstract.** If Sgr A* is a massive ($\sim 10^6\ M_\odot$) black hole embedded in a region with strong gaseous outflows, as suggested by stellar kinematic studies and the observation of He I, Br$\alpha$ and Br$\gamma$ line emission, it should be accreting from its environment via the Bondi-Hoyle process, unless it too is a source of powerful mass ejection. We discuss the consequences of this activity, including the expected mass and angular momentum accretion rate onto the black hole, and the resulting observable characteristics. The latest infrared images of this region appear to rule out the possibility that this large scale flow settles down into a standard $\alpha$-disk at small radii. We discuss some possible scenarios that might account for this, including strong advection in the disk or the presence of a massive, fossilized disk. Not all of the gas affected in this way by Sgr A*'s strong gravitational field becomes bound. Some of it is redirected into a focused flow that in turn interacts with other coherent gas structures near the black hole. We suggest that the mini-cavity (to the south-west of Sgr A*) may be formed as a result of this activity, and argue that the characteristics of the mini-cavity lend some observational support for the presence of a concentrated mass near Sgr A*. We show, however, that as far as the mini-cavity is concerned, this concentrated mass need not be in the form of a point mass, but may instead be a highly concentrated cluster of stellar remnants.

## 1. Introduction

The uniqueness of the radio source Sgr A*, together with its low proper motion ($< 40$ km s$^{-1}$; Backer & Sramek 1987) and its location near the dynamical center of the galaxy, suggest that it may be a massive point-like object dominating the gravitational potential in the inner 0.5 pc region. Its discovery followed a prediction that such an object might be visible at radio wavelengths (Lynden-Bell & Rees 1971), though the exact mechanism powering the radiative emission has been difficult to identify.

Over the past several years, however, multi-wavelength observations of the galactic center region have provided a much more detailed picture of the gas dynamics in the vicinity of Sgr A*, pointing to the accretion model as perhaps the

[1]Presidential Young Investigator

most likely physical process producing the spectral properties we now attribute to this blackhole candidate. Most, perhaps all, of Sgr A*'s radiative characteristics may be due to the energy liberated by a galactic center wind as it accretes down the deep potential well. This gaseous flow is inferred to have a velocity $v_w \approx 500-700$ km s$^{-1}$ and to constitute a mass loss rate $\dot{M}_w \approx 3-4\times10^{-3}\ M_\odot$ yr$^{-1}$ (Hall, Kleinmann & Scoville 1982; Geballe et al. 1991; Serabyn et al. 1991; Yusef-Zadeh & Melia 1991).

On the other hand, the nature of the Bondi-Hoyle accretion onto a point like object also presents somewhat of a challenge in understanding what happens to the gas as it settles down into a planar configuration close to the event horizon. Even if the ambient flow is uniform, fluctuations beyond the bow shock (located at roughly the accretion radius $R_{acc} \approx 10^5\ R_g$, where $R_g \equiv 2GM/c^2$ is the Schwarzchild radius) produce a transient accretion of net angular momentum that ought to result in the formation of a temporary (albeit small) disk. More realistically, the inflow itself carries angular momentum, so that the formation of a disk-like structure at small radii (i.e., $r \approx 10^{2-3}\ R_g$) is difficult to avoid. In this paper, we will discuss the characteristics expected of the large scale flow should Sgr A* be a point-like object with the mass ($\sim 1-2\times10^6\ M_\odot$; Haller et al. 1996) implied by the stellar kinematics, and we will consider several possibilities for the flow at smaller radii.

Coupled to this, is the question of whether the gaseous motions near Sgr A* are responsible for producing a feature known as the minicavity located in one of the ionized streamers (the Bar) appearing in radio continuum maps to the southwest of the dynamical center (Yusef-Zadeh, Morris & Ekers 1989). A chain of blobs of emission appearing in more recent, high-resolution radio images seem to lead away from Sgr A* toward the cavity, providing some morphological evidence that the two are physically connected. Spectroscopy and 1″ narrow-band imaging of near-infrared line emission in the central 0.3 pc of the Galaxy showed that the mini-cavity is a source of bright 2.2178$\mu$m line emission that has been unambiguously identified as [FeIII] (Lutz, Krabbe & Genzel 1994). This followed earlier detections of 2.217$\mu$m emission toward the Sgr A*/IRS 16 region by Eckart et al. (1992), who speculated that the radiation originates within an expanding bubble of ionized, hot iron driven by an outflow from the direction of the massive black hole candidate. This picture is supported by the derived fractional abundances of [Fe]/[H] $\geq 2.5\times10^{-5}$ and [Fe$^{++}$]/[Fe$^{+}$]$\approx$ 1 which, together with the observed spatial distributions and line profiles of [FeIII] and HI Br$\gamma$, suggest that an expanding gas bubble is being created in the partially neutral gas streamer by a fast ($\sim$ 1000 km s$^{-1}$) gas flow from one or several sources within a few arcsecs of the present location of the mini-cavity. Lutz et al. (1994) conclude that the most likely physical configuration of the mini-cavity is that of a shocked gas heated and compressed by this interaction, which destroys dust grains and releases iron into the gas phase. The dense postshock gas then forms an HII region, maintained at about 7000 K electron temperature via photoionization by the central UV field. The idea that dust is being destroyed is supported by the finding of Gezari & Yusef-Zadeh (1991) that the ratio of 12$\mu$m dust continuum to radio continuum flux has a minimum at the position of the mini-cavity.

Thus, in addition to considering the large scale infall onto the mass concentration near Sgr A*, we shall also address the issue of whether the "excess",

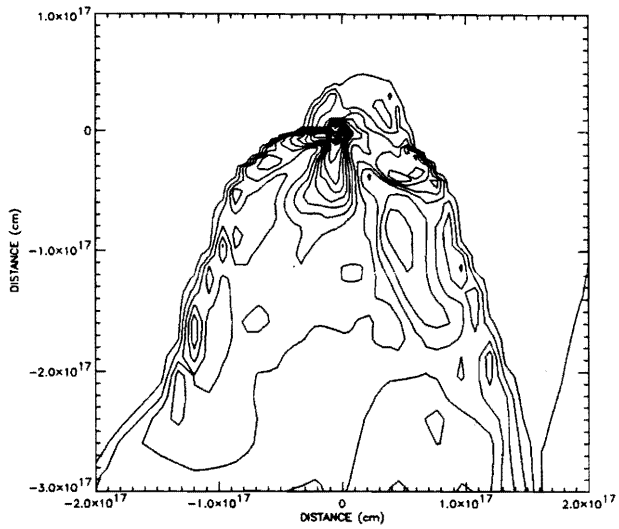


Figure 1. Cross-sectional contour plot of the density $\rho$ in the Bondi-Hoyle bow shock at Sgr A* (positioned at 0, 0). The image has 25 contours increasing as the square root of $\rho$ from $4.8 \times 10^3$ to $2.1 \times 10^5$ cm$^{-3}$. The galactic center wind entering from the top is described in the text and it flows past a black hole with mass $10^6$ $M_\odot$. The inner boundary is at 0.1 $R_{acc}$.

highly focused, hydrodynamic stream past Sgr A* has the correct distribution to be consistent with the gaseous flow required in the detailed modeling of the structure of the mini-cavity (Lutz et al. 1994). Knowing the IRS16 wind characteristics and Sgr A*'s mass provides an unambiguous profile of the collimated post-bow shock wind. We shall examine this situation both in the case where the mass concentration is in the form of a point-like object and where it is represented by a highly condensed cluster of stellar remnants. The latter may be of potential interest to an alternative scenario for the activity in this region, in which the concentrated mass may be in the form of a collapsed core in a cluster of white dwarfs (see, e.g., Haller et al. 1996). Although we make no attempt here to justify such a distribution on dynamical and evolutionary grounds, we do nontheless explore its viability in accounting for large scale features such as the minicavity. In this picture in which no massive black hole is present in the region, Sgr A* might then simply be the hot, magnetized gas trapped in the core of the stellar distribution, not unlike the X-ray emitting plasma in the potential well of clusters of galaxies (Melia & Haller 1996).

## 2. Bondi-Hoyle Accretion Onto Sgr A* and Radiative Emission

The length scale ($R_{acc}$) for accretion onto a compact object such as Sgr A* is set by determining the distance from the accretor at which the potential energy density of the flowing gas is matched to its kinetic energy density. In Figure 1 we show the cross-sectional density contours resulting from a 3-D hydrodynamic

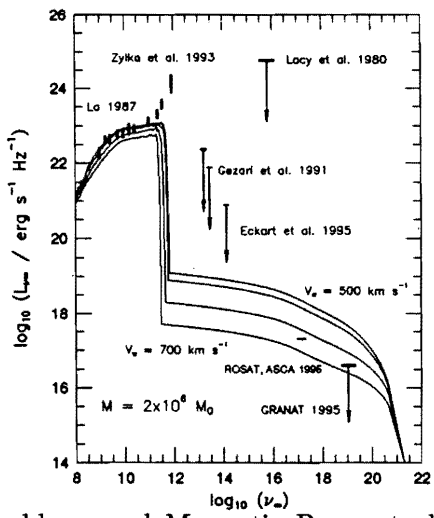


Figure 2. Bremsstrahlung and Magnetic Bremsstrahlung spectrum from the post bow-shock infall toward the black hole. The various curves range from a wind velocity of 500 km $s^{-1}$ (upper) to 700 km $s^{-1}$ (lower).

simulation with a domain of solution spanning a region of 30 $R_{acc}$ in either direction, using the black hole and galactic center wind characteristics discussed in § 1 above (see also Ruffert & Melia 1994; Melia, Coker & Yusef-Zadeh 1996; Coker & Melia 1996). Compression of the gas and magnetic field dissipation in the converging flow toward the black hole heat the gas, which in turn cools primarily by bremsstrahlung and magnetic bremsstrahlung emission with an emissivity characteristic of the particle density $n$, temperature $T$ and magnetic field intensity (Melia 1994). For the conditions in the galactic center, $n$ scales roughly as $r^{-3/2}$ with a value of about $2 \times 10^{11}$ $cm^{-3}$ at $r = R_g$, and $T$ varies from about $10^6$ K behind the shock to as high as $\sim 10^{10}$ K in the very inner region. Figure 2 shows the broad-band spectrum expected from this post-shock flow, in which the emissivity shortward of $\sim 10^{12}$ Hz is due primarily to thermal cyclotron/synchrotron radiation, whereas the flux at higher energies results from bremsstrahlung processes. In this figure, the ROSAT data point is consistent with the ASCA measurement when the $N_H \approx 2.2 \times 10^{23}$ $cm^{-2}$ of column density in the accreting flow is taken into account in estimating the line-of-sight absorption. Since the soft X-rays are produced gradually as the gas descends toward the event horizon, the overlying column density in the Bondi-Hoyle flow adds to the overall $N_H$ associated with this emission. We shall return to the question of what happens to this gas when it approaches the black hole in § 4.

## 3. Formation of the Mini-Cavity

The focused "excess" flow behind the accretor carries mass and mechanical energy flux into the Bar to the southwest of Sgr A*. In Figure 3, we show a

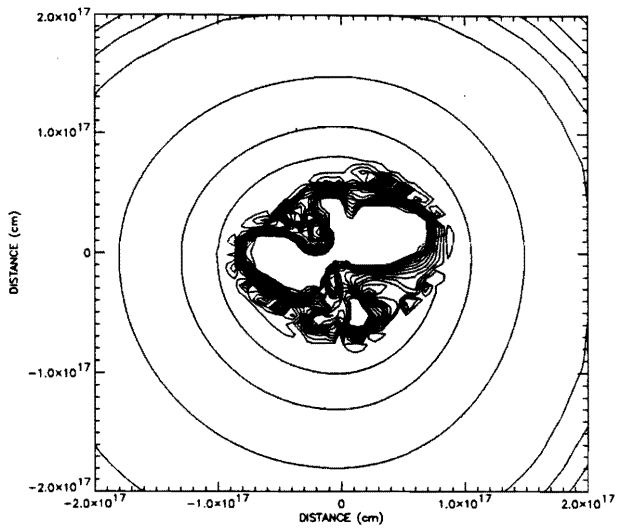


Figure 3. Cross-sectional contour map of the mechanical energy flux flowing into the minicavity. The image shows 20 contours increasing as the square root of the energy flux from 1,100 to 16,500 ergs cm$^{-2}$ s$^{-1}$. Note that the inner portion is low in flux due to the removal of the gas by accretion onto the black hole.

contour map of this kinetic energy flux perpendicular to the flow direction at the observed location of the minicavity. The radius of the post-bow shock flow corresponds very closely with the observed radius ($\sim 1''$, see Yusef-Zadeh et al. 1990) of the mini-cavity, suggesting that the energy required to dynamically control the activity in this hole is brought in by the mechanical flux. Indeed, Lutz et al. (1993) conclude in their detailed analysis of the cavity's emission that the power required to sustain its luminosity is $L_{cav} \approx 6 \times 10^{37}$ ergs s$^{-1}$ for reasonable values of the surrounding medium parameters. Our calculated value of the collimated flow's mechanical luminosity ($L_{shell} \approx 2.5\, L_{cav}$) is therefore about right to be the dominant energizing agent (Melia, Coker & Yusef-Zadeh 1996). We note that if the black hole mass is larger than the $\approx$ one million solar masses assumed here, then the focusing power of the accretor is greater and we would expect a larger mechanical luminosity and mass flux into the streamer. In addition, since the accretion radius scales as the mass, we would then also expect a larger size for the mini-cavity.

## 4. Accretion Onto the Black Hole

As one might guess by looking at the density profile in Figure 1, even when the upwind medium is uniform, the downwind region exhibits fluctuations in $\dot{M}$ that carry a net angular momentum down to the black hole. Detailed simulations (e.g., Ruffert & Melia 1994) suggest that at any given time, the accreting gas should circularize between 5 and 10 $R_g$. If the upwind medium has gradients in $\rho$ or $v_w$, as might arise from a distributed wind source, this circularization radius

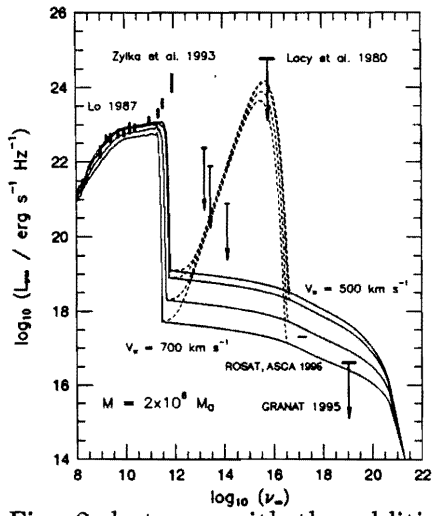


Figure 4. Same as Fig. 2, but now with the additional component (dotted curves) due to an $\alpha$-disk forming at smaller radii. The disk size and accretion rate are determined by the mass and angular momentum inflow rates from the Bondi-Hoyle shock.

might be even bigger. We have calculated the spectral component expected from a sum of blackbody emissions due to this disk (under the assumption that it is a standard $\alpha$ model), and show it as dotted curves in Figure 4. Since the infrared data are seemingly inconsistent with this additional spectral component, we conclude that either (1) the circularized flow does not form an $\alpha$-disk, but rather advects most of its dissipated energy through the event horizon (Narayan & Mahadevan 1995), (2) the Bondi-Hoyle flow merges into a massive, fossilized disk, storing most of the deposited matter at large radii (Falcke & Melia 1996), or (3) Sgr A* is not a point-like object (see below).

The first of these possibilities seems very promising. Every disk is advective to some degree. The question is whether the conditions in and around Sgr A* will permit a self-consistent disk solution with a very large advected fraction when the essential physics, including non-local effects and non-Keplerian flows, is incorporated into the analysis. In the second scenario, the wind infall must have a very large specific angular momentum, for it will otherwise settle onto the disk at small radii, where its kinetic energy will be thermalized and radiated away. A fossilized disk would thus need to function as a mass storage device, undergoing episodic accretion instabilities, not unlike those observed in X-ray Novae. The third possibility is discussed in the next section.

## 5. A Compact Cluster of Stellar Remnants ?

It is not unreasonable to presume that some 2−3 million white dwarfs could have formed and settled within the central cluster (Haller et al. 1996). Whether this distribution of stellar remnants could have undergone core collapse, however, is still not known. The reason this is of potential interest to our understanding of

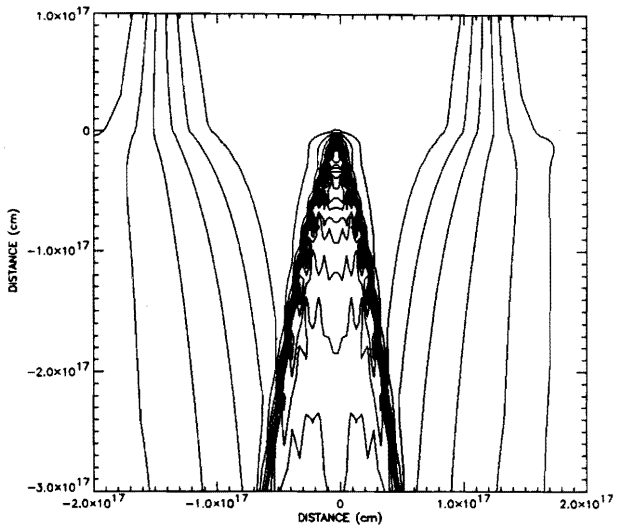


Figure 5. Gas condensation resulting from a Galactic center wind flowing past a cluster of $10^6$ one solar mass stellar remnants concentrated within a radius of $2R_{acc}$ at the location of Sgr A*. The image shows 25 contours scaling as the square root of the density from $1.3\times10^2$ to $7\times10^4$ cm$^{-3}$.

Sgr A* is that a concentration of $1-2$ million solar masses within $1-2$ $R_{acc}$ could in principle mimic the environmental impact of a point object. In that case, Sgr A* itself might simply be the trapped hot, magnetized plasma within the cluster (Melia & Haller 1996). We have carried out several 3D hydrodynamic simulations of a galactic center wind flowing through such a condensed (isothermal) cluster of one solar mass objects and the density profile of one of these is shown in Figure 5. Of course, unless the enclosed mass is $M_{cluster} = 2G/v_w^2\, R_{cluster}$, no shock will form since $R_{cluster}$ will then exceed $R_{acc}$. The case shown in Figure 5 is for $R_{cluster} = 2R_{acc}$. We see, however, that even in this case a condensation of the mass flow past the central mass has several features in common with the downwind Bondi-Hoyle flow we saw in Figure 1. When we examine the size and luminosity of the cavity produced in the Bar due to this type of flow (see Figure 6), the expected characteristics are not so different that we can immediately rule this picture out. To be sure, the minicavity should then be smaller and the luminosity is about half of the value we inferred in Figure 3. Nonetheless, this scenario is sufficiently intriguing that it merits further study. The most important test will be to see if the trapped gas can in fact account for the observed radio (and possibly X-ray) spectrum from this source.

**Acknowledgments.** This work was supported by NSF grant PHY 88-57218 and NASA grant NAGW-2822.

## References

Backer, D.B. & Sramek, R.A. 1987, in AIP Proc. 155, ed. D.B. Backer, 155

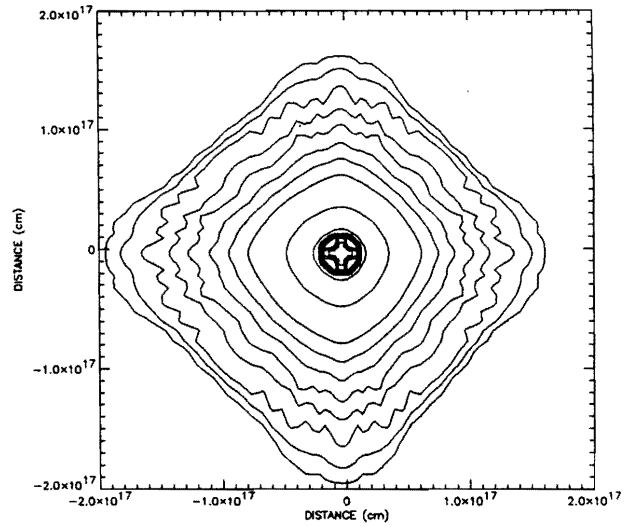


Figure 6. Cross-sectional contour map of the mechanical energy flux flowing into the minicavity for the case shown in Fig. 6. The image shows 20 contours increasing as the square root of the energy flux from 23 to 8,190 ergs $cm^{-2}$ $s^{-1}$.


Coker, R.F. & Melia, F. 1996, these proceedings.

Eckart, A., Genzel, R., et al. 1992, *Nature*, 355, 526

Eckart, A., et al. 1996, these proceedings

Falcke, H. & Melia, F. 1996, ApJ, submitted

Gezari, D. & Yusef-Zadeh, F. 1991, in Astrophysics with Infrared Arrays, ed. R. Elston, A. S. P. Conference Series Vol. 14, p. 214

Hall, D.N.B., Kleinmann, S.G. and Scoville, N.Z. 1982, ApJ, 260, L63

Haller, J.W., Rieke, M.J., Rieke, G.H., Tamblyn, P., Close, L. & Melia, F., 1996, ApJ, 456, 194

Lo, K.Y. 1987, in *AIP Proc. 155*, ed. D.C. Backer, (AIP: New York), 155, 30

Lutz, D., Krabbe, A. & Genzel, R. 1993, ApJ, 418, 244

Lynden-Bell, D. & Rees, M. 1971, MNRAS, 152, 461

Melia, F. 1994, ApJ, 426, 577

Melia, F., Coker, R.F. & Yusef-Zadeh, F. 1996, ApJ, 460, L33

Melia, F. & Haller, J.W. 1996, ApJ, in preparation

Narayan, R. & Mahadevan, R. 1995, *Nature*, 374, 623

Ruffert, M. & Melia, F. 1994, *A.A.*, 288, L29

Serabyn, E., Lacy, J.H., & Actermann, J.M. 1991, ApJ, 378, 557

Yusef-Zadeh, F. & Melia, F. 1991, ApJ, 385, L41

Yusef-Zadeh, F., Morris, M. & Ekers, R.D. 1990, *Nature*, 348, 45